Temperature dependence of the normal vibrational modes of hcp Zr

C. Stassis, J. Zarestky, D. Arch, O. D. McMasters, and B. N. Harmon
Ames Laboratory–United States Department of Energy and Departments of Physics and Metallurgy, Iowa State University, Ames, Iowa 50011
(Received 17 April 1978)

Inelastic-neutron-scattering techniques have been used to study the temperature dependence of the normal vibrational modes of hcp Zr. The phonon spectra along the [001], [100], and [110] symmetry directions were determined at 295, 773, and 1007 K. The [001] LO branch and a selected number of phonons of other branches were determined also at 5.5 K. As the temperature decreases we observe a rather large increase in the frequencies of all but the [001] LO branch. The zone-center mode of the [001] LO branch softens appreciably and at 5.5 K this branch exhibits a dip at the zone center reminiscent of the anomalous dispersion of the corresponding branch of technetium at room temperature. The data were used to evaluate the lattice specific heat at constant pressure as a function of temperature. The calculated total specific heat at constant pressure, obtained by taking into account the electronic contribution, was found to be consistent, to within experimental uncertainties, with the results of specific-heat measurements. We propose an explanation for the softening of the zone-center mode of the [001] LO branch and the large increase in the frequencies of the other modes with decreasing temperature which is based on the electronic structure of Zr.

I. INTRODUCTION

Pure zirconium metal solidifies at approximately 2123 K to a bcc structure (β phase) and undergoes to transformation of the martensitic variety to the hcp structure (α phase) at approximately 1135 K. At low temperatures ($\lesssim 0.5$ K) zirconium becomes superconducting. Zirconium, as well as Ti and Hf, exhibit some remarkable features in the temperature dependence of their electrical and thermodynamical properties. The electrical resistivity,[1] above room temperature, first increases linearly with temperature and then nearly saturates to a constant value. The heat capacity at constant pressure[2] for the hcp phase increases rapidly with temperature, and the elastic constants,[3] especially C_{66} and C_{44}, show a large decrease with increasing temperature. These characteristics have motivated numerous experimental and theoretical investigations regarding the temperature-dependent physical properties of these metals.

It has recently been suggested[4] that many of these features of the thermophysical properties of Ti, Zr, and Hf are anomalous and are caused by the decrease of the mean-free path of the conduction electrons to some limiting value (of the order of the atomic spacing) as the temperature is increased. The idea of a lower limit to the conduction-electron mean free path causing a negative deviation from linearity or saturation in the temperature dependence of the resistivity has been proposed previously.[5] However, the connection between such behavior in resistivity[6] or other anomalous thermophysical properties to a limited mean free path has not been clearly established. Measurements of the temperature dependence of the normal vibrational modes provides valuable information regarding the temperature dependence of the thermophysical properties of the metal.

In addition, measurements of the temperature dependence of the phonon dispersion curves of a metal provide information about the change with temperature of the electronic response to the nuclear motions and should help to clarify the physical picture emerging from recent microscopic models[7] of the lattice dynamics of metals. The effect of temperature is largest for electronic states near the Fermi level, and it is just these states which play the dominant role in screening and in coupling to the phonons in the superconducting state. For the superconducting hcp transition elements room-temperature measurements of the dispersion curves indicate that there is a correlation between the superconducting transition temperature T_c and the anomalous behavior of the zone-center [001] LO mode. The [001] LO branch of technetium,[8] which has the highest T_c (~ 8 K) of the hcp elements, exhibits a very pronounced dip at the zone center; in fact at the zone center the LO and TO branches have the same frequency, a degeneracy which is not required by symmetry. On the other hand the zone-center [001] LO mode of the low-T_c hcp transition elements is at room temperature only moderately softer than expected from the behavior of this mode in nonsuperconducting hcp elements. This can be seen, for instance, by comparing the room-temperature c-axis dispersion curves of Zr (Ref. 9) with those of Y (Ref. 10), which is not superconducting.

In this work we present the results of an experimental study of the temperature dependence of

the normal vibrational modes of hcp Zr. The phonon spectra along the [001], [100], and [110] symmetry directions were determined at 295, 773, and 1007 K. The [001] LO branch which was found to exhibit anomalous temperature dependence, and a selected number of phonons of other branches were determined also at 5.5 K. Preliminary results of this experiment were reported in an earlier communication.[11] In the present paper we present a complete report of these experiments.

II. EXPERIMENTAL DETAILS

The crystals used in the present experiments were prepared from a high-purity zirconium ingot obtained from the Teledyne Wah Chang Company. Analysis of a sample from the zirconium ingot showed that the hafnium content was less than 100 ppm. Large single crystals of Zr (3–4 cm^3 in volume) were grown by the following process. A cold-rolled sample of Zr, sealed in an evacuated tantalum crucible, was maintained for several hours at 1200 °C in a vacuum furnace, then cooled to 840 °C and maintained at this temperature for several days. After this heat treatment the sample was examined by standard neutron-diffraction techniques and the largest single crystal in the sample was separated by spark cutting.

The high-temperature measurements were performed using a vacuum furnace mounted on the sample goniometer of a triple-axis spectrometer. The sample was mounted between two tungsten heating elements, and two chromel-alumel thermocouples were used to control and measure its temperature. At approximately 800 °C the temperature was controlled to within a few degrees and the vacuum was approximately 10^{-5} Torr. In reaching the sample the neutron beam was traversing a 0.05-in. aluminum window and three 0.010-in. niobium heat shields. In the low-temperature measurements the sample was mounted in a conventional neutron-diffraction cryostat and its temperature (measured by a gold-iron thermocouple) at 5.5 K was controlled to within a few tenths of a degree.

The measurements were performed using a triple-axis spectrometer at the 5-MW Ames Laboratory Research Reactor. All data were collected using the constant-Q method, where Q denotes the neutron scattering vector. A variable incident neutron energy and, whenever possible, a fixed scattered-neutron energy of 13.6 meV were used. Pyrolitic graphite was used as a monochromator and analyzer, and a pyrolitic graphite filter was placed in the scattered beam to attenuate higher-order contaminations. In some instances scattered neutron energies of up to 27 meV were used to avoid spurious peaks due to higher-order contaminations. At each temperature the lattice constants of the crystal were assessed by measuring the scattering angles of appropriate Bragg reflections in the scattering plane. The change with temperature of the lattice constants of the crystal are in good agreement with thermal-expansion measurements.[12]

III. EXPERIMENTAL RESULTS

The phonon-dispersion curves were determined along the [001], [100], and [110] symmetry directions at 295, 773, and 1007 K. The [001] LO branch as well as a selected number of phonons of other branches were also obtained at 5.5 K. The measured phonon frequencies are listed in Table I and the experimental dispersion curves are plotted in Figs. 1–3. The room-temperature data along the [100] and [001] direction are in good agreement with previous measurements[9] of the dispersion curves along these directions. Also, our data for the [100] TA($\|$) branch are in good agreement with the measurements of Moss *et al.*[13]

It can be seen (Table I and Figs. 2 and 3) that the frequencies of all branches except the [001] LO branch whose anomalous behavior will be discussed later in this section, decrease with increasing temperature. In general one would expect the phonon frequencies to decrease as the volume increases with increasing temperature. However, the observed frequency shifts are relatively large and cannot be accounted for solely by the effect on the vibrational frequencies of the thermal expansion of the lattice. The frequency shifts due to the latter effect, estimated using the thermodynamic Grüneisen parameter,[12] are approximately seven times smaller than the experimentally observed frequency shifts. This observation implies that the observed frequency shifts are mainly due to an explicit temperature dependence of the phonon frequencies. This conclusion is consistent with the results of measurements[14] of the pressure dependence of the elastic constants of zirconium.

The largest frequency shifts observed in the present experiment are of the order of 10%. Measurements[3] of the temperature dependence of the elastic constants of zirconium, on the other hand, show that the softening of the frequencies near $q = 0$ with increasing temperature is much more pronounced for some branches. In particular, the elastic constant measurements imply a decrease of the slope of the [100] TA($\|$) branch by almost a factor of 2. Therefore, the decrease

TABLE I. Measured frequencies (meV) of hcp Zr. The symbols ⊥ and ∥ refer to polarization perpendicular and parallel to the basal plane, respectively.

TA [00ξ]

ξ	$T=5.5$ K	$T=295$ K	$T=773$ K	$T=1007$ K
0.10		1.86±0.04	1.41±0.12	1.36±0.04
0.20		3.43±0.04	3.18±0.08	2.98±0.04
0.25		4.22±0.08		
0.30		4.92±0.04	4.63±0.08	4.38±0.08
0.40		6.37±0.08	5.91±0.08	5.67±0.08
0.50	7.86±0.17	7.49±0.08	6.95±0.17	6.70±0.17

LO [00ξ]

ξ	5.5 K	295 K	773 K	1007 K
0	17.50±0.62	19.07±0.17	20.14±0.33	20.10±0.25
0.10	18.41±0.41	18.94±0.25		20.27±0.33
0.20	18.61±0.41	18.98±0.25	18.32±0.62	19.52±0.33
0.30	19.23±0.41	19.07±0.33	19.52±0.50	19.60±0.33
0.40	18.20±0.33			18.41±0.33
0.50	17.37±0.21	17.16±0.25	16.83±0.12	16.67±0.12

TO [00ξ]

ξ	5.5 K	295 K	773 K	1007 K
0	11.00±0.08	10.59±0.12	9.60±0.62	8.93±0.25
0.10		10.59±0.12	9.26±0.21	8.60±0.17
0.20		9.97±0.12	8.89±0.17	8.27±0.12
0.30		9.14±0.08	8.31±0.17	7.98±0.17
0.40		8.44±0.08	7.82±0.12	7.44±0.12
0.50	7.86±0.17	7.49±0.08	6.95±0.17	6.70±0.17

TA(⊥) [ξ00]

ξ	5.5 K	295 K	773 K	1007 K
0.10		3.23±0.04	2.94±0.08	2.77±0.04
0.15		4.88±0.04		
0.20		6.49±0.04	5.79±0.08	5.42±0.04
0.30		9.14±0.08	8.27±0.08	7.78±0.04
0.40		10.84±0.08	9.97±0.12	9.51±0.12
0.50		11.29±0.17	10.88±0.21	10.26±0.17

LA [00ξ]

ξ	5.5 K	295 K	773 K	1007 K
0.10		4.18±0.12	3.97±0.12	3.93±0.12
0.20		8.02±0.12	7.65±0.17	7.53±0.08
0.30		11.66±0.12	11.13±0.17	10.92±0.12
0.40				14.39±0.17
0.50	17.37±0.21	17.16±0.25	16.83±0.12	16.67±0.12

LA [ξ00]

ξ	5.5 K	295 K	773 K	1007 K
0.10		6.95±0.12	6.33±0.21	6.33±0.08
0.20		13.36±0.12	12.45±0.25	11.95±0.17
0.30		17.29±0.12	16.71±0.41	16.42±0.17
0.40				19.15±0.25
0.50		21.26±0.17	19.77±0.41	19.56±0.33

TA(∥) [ξ00]

ξ	5.5 K	295 K	773 K	1007 K
0.10		3.43±0.04		
0.20		6.33±0.04		
0.30		8.15±0.25		
0.40		9.14±0.12		
0.50		9.64±0.25		

LO [ξ00]

ξ	5.5 K	295 K	773 K	1007 K
0	11.00±0.08	10.54±0.12	9.60±0.62	8.93±0.25
0.10				11.42±0.41
0.20		17.25±0.25	14.56±0.83	14.89±0.62
0.30		20.76±0.25		
0.40		21.96±0.25	20.02±0.74	19.69±0.62
0.50		22.17±0.21	20.80±0.62	21.34±0.62

TO(⊥) [ξ00]

ξ	5.5 K	295 K	773 K	1007 K
0	17.95±0.62	19.07±0.17	20.14±0.33	20.10±0.25
0.10		19.03±0.21		20.10±0.33
0.20				19.81±0.33
0.30		19.65±0.29	19.48±0.41	19.48±0.41
0.40				19.11±0.41
0.50		20.06±0.32	19.36±0.41	18.45±0.33

TA(⊥) [ξξ0]

ξ	5.5 K	295 K	773 K	1007 K
0.05		2.94±0.04		
0.10		5.79±0.04		4.84±0.08
0.20		10.46±0.08		9.18±0.17
0.30		14.52±0.17		
0.33		16.05±0.33		15.22±0.25
0.40		18.69±0.25		17.33±0.41
0.50		19.94±0.25		18.12±0.25

TO(∥) [ξ00]

ξ	5.5 K	295 K	773 K	1007 K
0	11.00±0.08	10.59±0.12		
0.10		12.33±0.08		
0.20		14.85±0.17		
0.30		17.70±0.21		
0.40				
0.50		19.44±0.25		

LA [ξξ0]

ξ	5.5 K	295 K	773 K	1007 K
0.05		6.20±0.08		
0.10		10.88±0.17		
0.20		15.30±0.25		
0.33		17.87±0.41		
0.40		18.82±0.25		
0.45		19.11±0.25		
0.50		19.44±0.25		

TABLE I. (*Continued*).

TA(∥) [ξξ0]					TO(∥) [ξξ0]				
ξ	5.5 K	295 K	773 K	1007 K	ξ	5.5 K	295 K	773 K	1007 K
0.05		3.23 ± 0.04			0		10.67 ± 0.33		
0.10		6.66 ± 0.08			0.10		14.48 ± 0.17		
0.20		13.15 ± 0.08			0.15		18.24 ± 0.17		
0.30		14.89 ± 0.41			0.20		20.43 ± 0.25		
0.35		15.30 ± 0.25			0.30		20.68 ± 0.41		
0.40		13.98 ± 0.25			0.35				
0.45		10.75 ± 0.25			0.50		22.17 ± 0.21	20.80 ± 0.62	21.34 ± 0.62
0.50		9.10 ± 0.17							
TO(⊥) [ξξ0]					LO [ξξ0]				
ξ	5.5 K	295 K	773 K	1007 K	ξ	5.5 K	295 K	773 K	1007 K
0		19.11 ± 0.33		20.10 ± 0.33	0		10.67 ± 0.33		
0.10		19.11 ± 0.33		19.56 ± 0.33	0.05		12.61 ± 0.41		
0.20		19.40 ± 0.33			0.10		16.13 ± 0.21		
0.30		17.37 ± 0.25			0.15		19.19 ± 0.17		
0.33		16.21 ± 0.33		15.22 ± 0.25	0.20		20.43 ± 0.25		19.65 ± 0.33
0.40		12.90 ± 0.41		11.45 ± 0.25	0.30		19.19 ± 0.33		
0.50		11.04 ± 0.25		9.84 ± 0.25	0.45		20.47 ± 0.50		
					0.50		21.26 ± 0.17	19.77 ± 0.41	19.56 ± 0.33

in the frequencies of the phonon modes of zirconium is more pronounced in the limit of long-phonon wavelengths. This observation suggests that the frequency shifts are due to changes in the long-range interatomic forces which are mainly determined by the electronic response to the nuclear motions.

With increasing temperature no significant systematic changes in the phonon widths were observed, which is surprising in view of the rather large shifts in the phonon frequencies. Thus, as the hcp→bcc transformation temperature was approached from below, we did not observe any dramatic changes either in the widths or the frequencies of the vibrational modes. This suggests that the hcp→bcc transition in zirconium is of the first order.

The most interesting aspect of the data is the anomalous temperature dependence of the [001] LO branch. It can be seen (Fig. 3) that as the

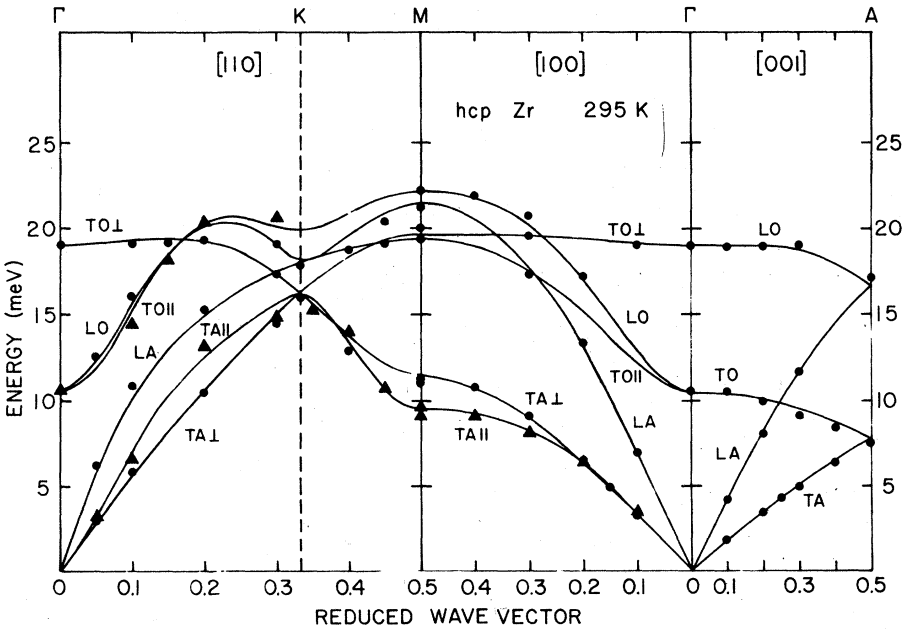

FIG. 1. Phonon dispersion curves of hcp Zr along the [001], [100], and [110] symmetry directions at 295 K. The solid lines were obtained by fitting the data to the force-constant model of DeWames *et al.* (Ref. 19).

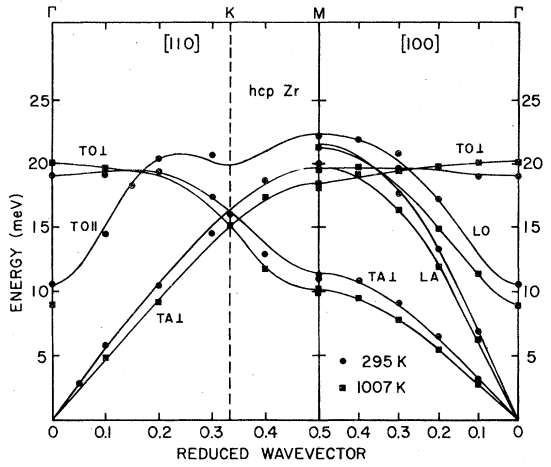

FIG. 2. Phonon dispersion curves of hcp Zr along the [100] and [110] symmetry directions at 295 and 1007 K.

temperature decreases the zone-center mode of the [001] LO branch softens significantly, and at 5.5 K this branch exhibits a dip at the zone center. This behavior is similar but not as pronounced as the anomalous dispersion exhibited at room temperature by the corresponding branch of technetium[8] which has the highest superconducting transition temperature ($T_c \sim 8$ K) of the hcp elements.

Within the framework of the force-constant models of lattice dynamics the temperature dependence of the phonon frequencies is attributed to the anharmonic terms of the crystal potential. Once these terms have been obtained from the experimental data, the anharmonic contribution to the specific heat (and other thermodynamic properties of the solid) can be evaluated. However, at intermediate temperatures the expressions for the anharmonic terms involve so many parameters that the calculations can be carried out only by assuming relatively simple forms for the interatomic potential. In the following analysis we will adopt an alternative approach in which the specific heat is calculated from a general expression for the entropy of the solid.

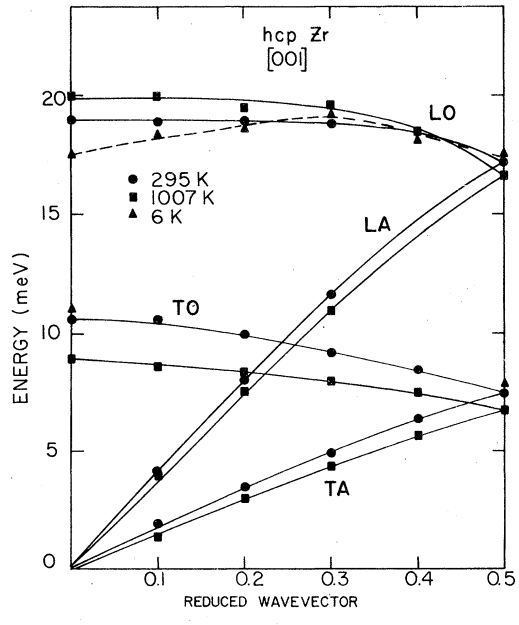

FIG. 3. Temperature dependence of the dispersion curves of hcp Zr along the [001] direction.

IV. LATTICE SPECIFIC HEAT

In most cases of interest the lattice contribution to the entropy of a solid $S^{(l)}$ can be calculated from the usual harmonic expression for the entropy,

$$S^{(l)} = -k \sum_{\sigma} [n_\sigma \ln(n_\sigma) - (1+n_\sigma)\ln(1+n_\sigma)], \qquad (1)$$

where

$$n_\sigma = (e^{\beta\hbar\omega_\sigma} - 1)^{-1},$$

$\beta = 1/kT$, k is the Boltzmann constant, and σ stands for $(\vec{q}, j)$, the wave vector and branch index of the mode. It is important to point out that in general the quasiparticle frequencies ω_σ appearing in Eq. (1) are not the same as the dynamic frequencies determined by neutron spectroscopy. However, it has been shown[15,16] that Eq. (1) with frequencies ω_σ determined by inelastic neutron scattering techniques is valid in two important cases: (a) within the quasiharmonic approximation and (b) to leading order in the usual anharmonic perturbation theory. Actually it is widely believed that, even if the above conditions are not fulfilled, Eq. (1) with ω_σ replaced by the frequencies determined by neutron spectroscopy can be used to accurately evaluate the thermodynamic properties at constant pressure of the solid. In this form Eq. (1) has been used to calculate the thermodynamic properties of Nb,[17] and Cu and Pd,[18] from data obtained from inelastic neutron scattering experiments. In the following analysis we adopt Eq. (1) with the frequencies ω_σ replaced by the experimentally determined frequencies.

From Eq. (1) the specific heat at constant pressure $C_P^{(l)}$ is

$$C_P^{(l)} = Nk \sum_{\sigma} \frac{x_\sigma^2}{\sinh^2 x_\sigma} \left[1 - \left(\frac{\partial \ln(\omega_\sigma)}{\partial \ln T}\right)_p\right], \qquad (2)$$

where $x_\sigma = \hbar\omega_\sigma/2kT$. The first term is the quasi-

harmonic contribution $C_P^{(1)}$(QH) and the second arises from the explicit temperature dependence of the frequencies. Notice that at the high temperature limit $x_\sigma \ll 1$,

$$C_P^{(1)} \simeq 3Nk\left[1-\left(\frac{\partial\langle\ln\omega\rangle}{\partial \ln T}\right)_p\right], \tag{3}$$

where

$$\langle\ln\omega\rangle = \int g(\omega, T)\ln\omega\, d\omega \tag{4}$$

and $g(\omega, T)$ is the frequency distribution at temperature T. Thus in order to evaluate the specific heat at constant pressure the frequencies and their temperature derivatives are needed at each temperature. Since only the frequencies of a small number of modes are measured at a few temperatures appropriate interpolation schemes are required for the analysis of the experimental data. The frequencies at a given temperature are generated throughout the appropriate section of the Brillouin zone by fitting the experimentally measured frequencies to a Born–von-Kármán force model. In order to evaluate the temperature derivatives of the frequencies the interpolation scheme used by Miiller and Brockhouse[18] in their calculation of the thermodynamic properties of Cu and Pd has been adopted. In this scheme the temperature dependence of the normal modes is given by

$$\omega_\sigma(T) = \omega_\sigma(T_1) f(T), \tag{5}$$

where T_1 is a reference temperature and $f(T)$, the average temperature dependence of the modes, is obtained from the experimental data,

$$f(T) \equiv \left\langle \frac{\omega_\sigma(T)}{\omega_\sigma(T_1)} \right\rangle = \frac{1}{n}\sum_\sigma^n \frac{\omega_\sigma(T)}{\omega_\sigma(T_1)}, \tag{6}$$

where n is the total number of modes measured at the temperatures T_1 and T. Using Eq. (5) with Eq. (2) the specific heat at constant pressure can be obtained at a given temperature from the frequency distribution at the reference temperature T_1,

$$C_P^{(1)} = 3Nk\left(1 - T\frac{f'(T)}{f(T)}\right)\int g(\omega, T_1)\frac{x^2}{\sinh^2[xf(T)]}d\omega. \tag{7}$$

In the analysis of the experimental results the frequency spectrum at room temperature ($T_1 = 295$ K) will be used.

The data in the present experiment were fitted using the modified axially symmetric force constant model of DeWames *et al.*[19] In this force-constant model interatomic interactions are included out through sixth nearest neighbors and the interaction for a given shell of neighbors is specified in terms of one bond-stretching constant and two bond-bending constants. Thus there are 18 force constants to be determined by fitting the experimental results by this model. As can be seen from Fig. 1, this model provides a satisfactory fit to the experimentally determined dispersion curves. The force constants for the room-temperature data are listed in Table II. Using these force constants, the frequency distribution at room temperature, which will be used for calculating $C_P^{(1)}$ [Eq. (7)], was evaluated by the interpolation method of Raubenheimer and Gilat[20] and is plotted in Fig. 4.

The lattice specific heat at constant pressure was calculated from Eq. (7) using the room-temperature ($T_1 = 295$ K) frequency distribution with the average-mode temperature dependence determined from Eq. (6). Since the experimentally determined frequencies vary, to within experimental errors, linearly with temperature (Fig. 5) the averaging by Eq. (6) determines the average slope of this linear dependence. In order to ascertain whether adopting an average temperature dependence is an appropriate interpolation

TABLE II. Force constants (10^3 dyn/cm) obtained by fitting the 295-K data of hcp Zr to the DeWames *et al.* (Ref. 19) model. These force constants were utilized to obtain the room-temperature frequency distribution (Fig. 4) by the interpolation method of Raubenheimer and Gilat (Ref. 20). The notation is that of DeWames *et al.* (Ref. 19).

$K(1, 1-2)$	39.74
$C_{B_x}(1, 1-2)$	−3.77
$C_{B_z}(1, 1-2)$	−12.88
$K(2, 1-1)$	22.80
$C_{B_x}(2, 1-1)$	−0.70
$C_{B_z}(2, 1-1)$	3.28
$K(3, 1-2)$	−4.60
$C_{B_x}(3, 1-2)$	−0.39
$C_{B_z}(3, 1-2)$	−1.45
$K(4, 1-1) + C_{B_z}(4, 1-1)$	8.40
$C_{B_x}(4, 1-1)$	0.43
$K(5, 1-2)$	1.95
$C_{B_x}(5, 1-2)$	0.28
$C_{B_z}(5, 1-2)$	−0.26
$K(6, 1-1)$	1.48
$C_{B_x}(6, 1-1)$	1.71
$C_{B_z}(6, 1-1)$	0.10

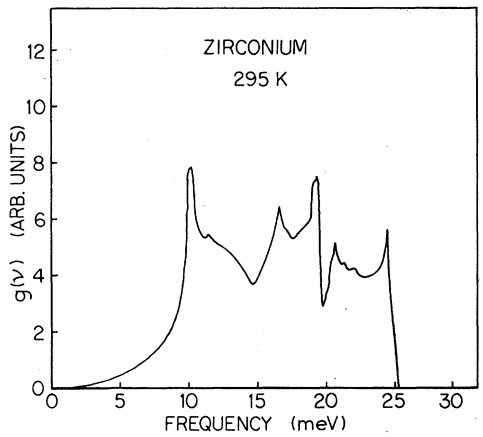

FIG. 4. Phonon spectrum of hcp Zr at 295 K.

scheme (in particular in view of the anomalous temperature dependence of the [001] LO branch) we performed several calculations to assess its validity. First the lattice specific heat was evaluated at 773 and 1007 K using Eq. (3), which provides a fair approximation for the specific heat at these temperatures. The average value of $\ln\omega$ was evaluated using the frequency distributions at 295, 773, and 1007 K and was found (Fig. 6) to vary linearly with temperature. The lattice specific heat evaluated using the slope of $\langle\ln\omega\rangle$ was found to agree to better than 2% with that calculated using an average temperature dependence for the normal modes. As an additional test of the interpolation scheme we performed an analysis of our data using the quasiharmonic approximation.[21] In this scheme, valid for small frequency shifts (a condition satisfied in the present experiment), the measured frequencies are written as

$$\omega_\sigma(T) = \omega_\sigma^{(h)} + \Delta_\sigma(T), \tag{8}$$

where $\Delta_\sigma(T)$ are the frequency shifts from the harmonic frequencies $\omega_\sigma^{(h)}$. Using Eq. (1) the change in entropy due to the explicit temperature dependence of the frequencies can be written as

$$\Delta S^{(1)} = -\hbar \sum_\sigma \left(\frac{\partial n_\sigma}{\partial T}\right) \Delta_\sigma(T), \tag{9}$$

where the occupational numbers n_σ are evaluated at the harmonic frequencies $\omega_\sigma^{(h)}$. Since the frequencies observed in the present experiment vary, to within experimental errors, linearly with temperature (Fig. 5) the harmonic frequencies $\omega_\sigma^{(h)}$ were obtained by extrapolating to 0 K. The harmonic frequencies obtained in this manner were found to agree to within experimental errors with the frequencies measured at 5.5 K. The specific heat was evaluated using Eq. (9) to obtain the contribution due to the explicit temperature

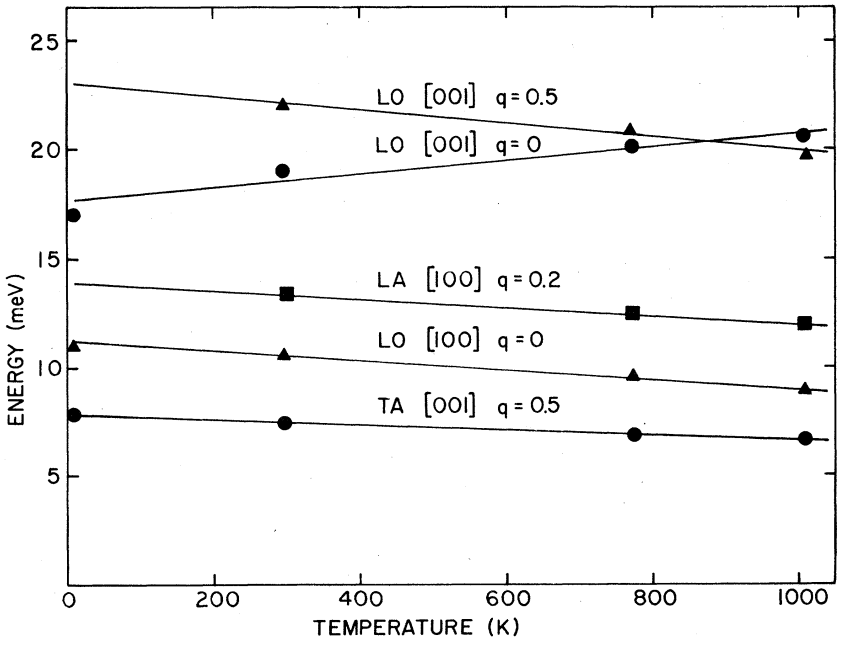

FIG. 5. Temperature dependence of the frequencies of some normal modes of hcp Zr.

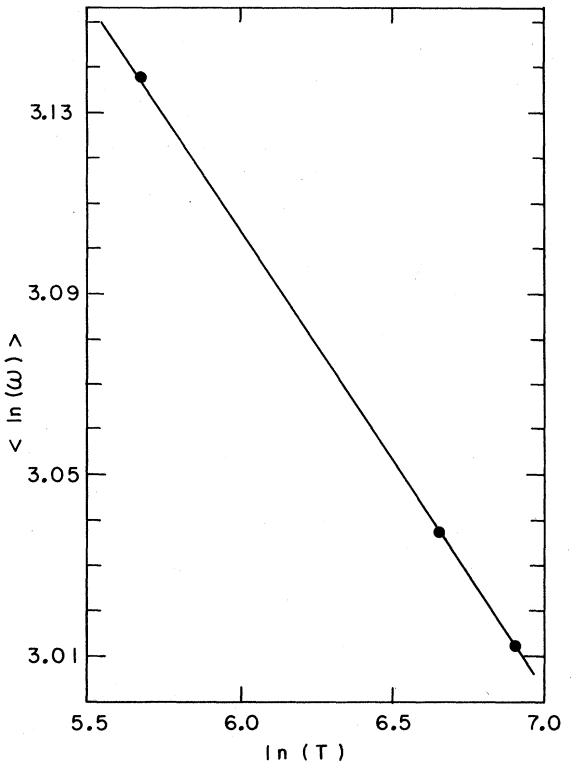

FIG. 6. Temperature dependence of $\langle \ln\omega \rangle$ evaluated using Eq. (4).

dependence of the frequencies and the harmonic contribution was obtained using the frequency distribution determined by the frequencies $\omega_\sigma^{(h)}$. The specific heat evaluated using this approach was found to agree to better than 2% with that obtained using the interpolation scheme of Miiller and Brockhouse. Since both Eqs. (3) and (9) involve approximations, a much more stringent test of the validity of the interpolation scheme of Miiller and Brockhouse is to evaluate the entropy directly from Eq. (1) at 295, 773, and 1007 K using the measured frequency spectra. The values of entropy obtained by this direct calculation agree to within 1% at 773 K and to within 4% at 1007 with the values obtained by the interpolation scheme of Miiller and Brockhouse.

The calculated lattice specific heat $C_P^{(l)}$ is compared in Fig. 7 with $C_P^{(l)}$(QH), the quasiharmonic lattice specific heat [given by the first term of Eq. (2)], which approaches the classical value at high temperatures. It can be seen that there is a large contribution arising from the explicit temperature dependence of the phonon frequencies [the second term of Eq. (2)]. In order to compare with the experimental C_P values the

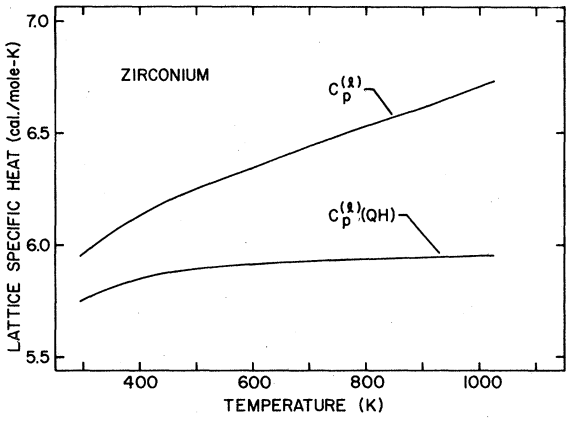

FIG. 7. Temperature dependence of the lattice specific heat at constant pressure $C_p^{(l)}$ evaluated using the Miiller-Brockhouse interpolation scheme (Ref. 18). C_p^l(QH) is the quasiharmonic lattice specific heat given by the first term of Eq. (2).

electronic specific heat was evaluated using the electronic density of states obtained by a band-theoretical calculation and is shown in Fig. 8. Note that the calculated $C_V^{(e)}$ is considerably higher at high temperatures than that obtained by the usual linear extrapolation from low temperatures. This is due to the increase with increasing temperature of the effective density of states at the Fermi level. The electronic contributions to the specific heat obtained from our band-theoretical calculation of the electronic density of states (Fig. 8) is considerably lower than that estimated by Shimizu and Katsuki[22] using a density-of-states determined from the low-temperature specific-heat data of 4*d* metals and their alloys. The higher values for the electronic specific heat obtained by Shimizu and Katsuki may be due to the

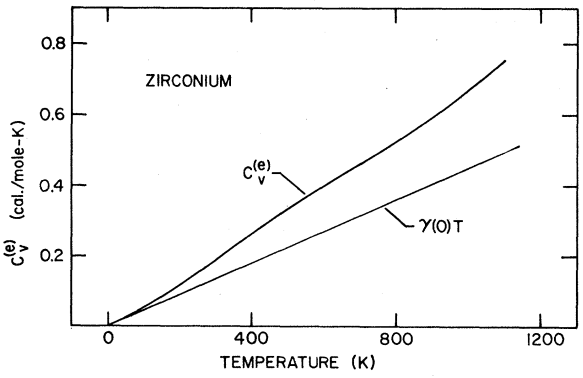

FIG. 8. Electronic contribution to the specific heat $C_V^{(e)}$ evaluated using the electronic density of states shown in Fig. 10. $\gamma(0)T$ is the linear extrapolation from low temperatures.

electron-phonon enhancement which is included in their empirical density of states. Note that at temperatures higher than about twice the Debye temperature the electron-phonon mass enhancement is negligible,[23] so that our use of the bare density of states to calculate $C_v^{(e)}$ should be valid. The calculated total specific heat at constant pressure is compared in Fig. 9 with the experimental values of C_P obtained by various workers.[2,24-26] The agreement is quite satisfactory in view of the large discrepancies (of the order of 10%) in the values of the specific heat measured by various workers. We may therefore conclude that the temperature dependence of the normal vibrational modes of hcp Zr as measured in the present experiment is consistent with the observed thermodynamic properties.

V. DISCUSSION

In Sec. IV we showed that the temperature dependence of the normal vibrations of Zr observed in the present experiment is consistent to within experimental uncertainties with the high-temperature characteristics of the measured specific heat. A more fundamental understanding, however, of the experimental results, in particular of the anomalous temperature dependence of the [001] LO branch, could be obtained only within the framework of the microscopic theory of lattice dynamics. Although in the last few years considerable progress has been achieved in this direction, a microscopic theory suitable for realistic calculations at finite temperatures is not presently available. In the following we discuss the experimental results using a microscopic model, proposed recently by Sinha and Harmon,[7] which establishes the connection between the electronic structure of the d-band metals and the charge-density fluctuations induced by the vibrational motions of the nuclei.

In this model the anomalous dips in the phonon spectrum of Nb can be understood as arising from the coupling of monopolar charge fluctuations within the d-band complex near the Fermi energy with the longitudinal lattice vibrations. However, in Zr such monopolar charge fluctuations do not couple to the zone-center mode of the [001] LO branch. This mode, on the other hand, does couple strongly to dipolar fluctuations of the charge density, as suggested by the success of the shell model in fitting the anomalous dispersion curves of technetium along the [001] direction.[27]

In a metal the magnitude and spatial character of the conduction-electron response is largely determined by the density and type of states near the Fermi level—properties which are described formally by the generalized susceptibility function.[7] For the induced charge density to have significant odd parity or dipolar spatial character, it is favorable that the wave functions near E_F be states of mixed parity (i.e., an angular momentum

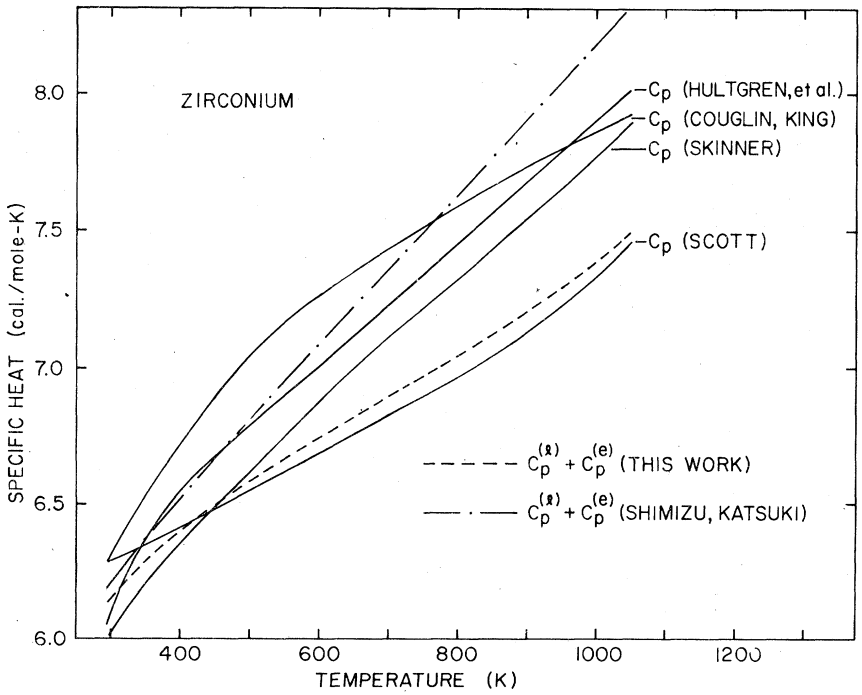

FIG. 9. Comparison of the specific heat at constant pressure C_p obtained by adding $C_p^{(e)}$ to $C_p^{(l)}$ with the experimental results obtained by various workers (Refs. 2 and 22–24). The dashed and point-dashed lines are the specific heats obtained by using the electronic contribution evaluated in this work and by Shimizu and Katsuki (Ref. 22), respectively.

decomposition of the Bloch states about an atomic site must contain s and p, p and d, or d and f character). Just such a favorable situation occurs in the electronic states of zirconium. The fifth and sixth bands near the point H fall just below E_F and contain a large admixture of both p and d character. This has been determined by our recent calculation of the wave functions and band structure of Zr. The results of these calculations are similar to those obtained by Jepsen *et al.*[28] The density of states (DOS) from our calculation is shown in Fig. 10. The small peak in the DOS just below E_F arises from the bands near H, while the large increase in the DOS just above E_F arises from bands with pure d character.

At low temperatures all the states with p character near H are occupied and give rise to strong screening of the [001] LO branch near $q=0$ due to dipolar fluctuations. Raising the temperature has two important effects: (a) the p character near the Fermi level is depleted, causing a decrease in the dipolar fluctuations and hardening of the zone-center LO phonons; and (b) the effective density of states at the Fermi level is increased due to the large peak in the d-like density of states just above E_F. This latter effect will add to the usual metallic screening of the bare Coulomb interaction between ions and lead to a general decrease in phonon frequencies. This metallic screening can be interpreted as a decrease of the force constants with increasing temperature as suggested by Grimvall,[4] and helps explain the high-temperature heat-capacity results. That the effective density of states at the Fermi level increases can be seen directly in the calculated electronic heat capacity. A constant density of states would yield a straight line $\gamma(T=0)T$, whereas the actual curve (Fig. 8) shows that $\gamma(T)$ increases with temperature and corresponds at 1000 K to an increase in the effective density of states of 35%.

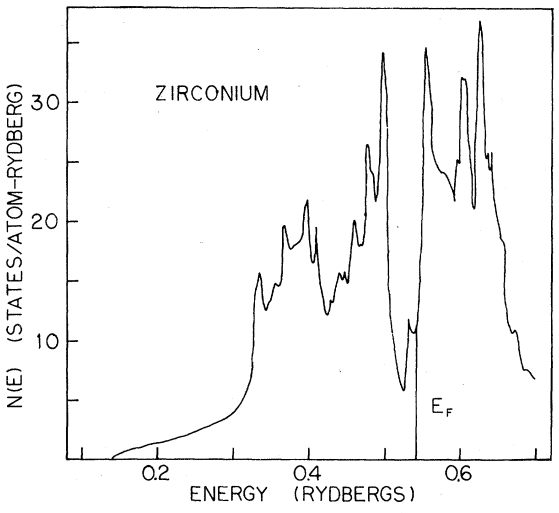

FIG. 10. Density of electronic states used for the calculation of $C_V^{(e)}$.

We should also remark that the same p-d character near E_F which enhances the dipolar fluctuations would also favor strong electron-phonon matrix elements and help promote superconductivity. A reasonable and simple approximation for the electron-phonon matrix elements is the so-called "rigid-ion" approximation which involves matrix elements of the form $\langle\psi_{\vec{k}}|\nabla\vec{\nabla}|\psi_{\vec{k}'}\rangle$, where V is the single-site muffin-tin potential used in the band-structure calculation. Again because of the rules for tensor coupling a wave function ψ_k with angular-momentum character l can only couple to the $l\pm1$ components of the wave function $\psi_{k'}$. The relevant states for superconductivity are at the Fermi level where substantial p and d character of the wave functions occurs. This may explain the correlation between the dips in the [001] LO branch and the superconducting temperatures.

The details of the model we describe above are somewhat speculative. For example, the p and d character of the wave functions near E_F could also couple and give rise to a charge density with strong $l=3$ character. To obtain a definitive confirmation of our proposed model we are presently performing first-principles band-structure calculations for the electronic structure of a frozen phonon lattice in which the two atoms in the unit cell are 5% closer along the c axis. We are also investigating the connection between the results of the present experiment and the recent theoretical model of Varma and Weber.[7]

Preliminary experimental results on hcp Ti show that the temperature dependence of the normal vibrational modes of this metal is similar to that of Zr; in particular the zone center mode of the [001] LO branch softens with decreasing temperature. This is what one would expect from the similarity of the electronic structures of Ti and Zr.

ACKNOWLEDGMENTS

This work was supported by the U. S. Department of Energy, Office of Basic Energy Sciences, Materials Sciences Division. The authors are grateful to S. Liu and N. Wakabayashi for many useful discussions.

[1]J. L. Wyatt, Trans. AIME 197, 903 (1953); L. A. Cook, L. S. Castleman, and W. E. Johnson, Westinghouse Corporation Report WAPD-25, 1950 (unpublished).
[2]See, for instance, R. Hultgren, P. D. Desai, D. T. Hawkins, M. Gleiser, K. K. Kelley, D. D. Wagman, *Selected Values of the Thermodynamic Properties of Elements* (American Society for Metals, Cleveland, 1967), and references therein.
[3]E. S. Fisher and C. J. Renken, Phys. Rev. 135, A482 (1964).
[4]G. Grimvall, in *Proceedings of the International Conference on the Physics of Transition of Metals, Toronto, August* 1977 (The Institute of Physics, Bristol and London, 1977),
[5]A. F. Ioffe and A. R. Regel, Prog. Semicond. 4, 237 (1960); N. F. Mott and E. A. Davis, *Electronic Processes in Non-Crystalline Materials* (Clarendon, Oxford, 1971); P. B. Allen, Phys. Rev. Lett. 37, 1638 (1976).
[6]M. J. Laubitz, C. R. Leavens, and R. Taylor, Phys. Rev. Lett. 39, 255 (1977).
[7]S. K. Sinha and B. N. Harmon, Phys. Rev. Lett. 35, 1515 (1975); M. Gupta and A. J. Freeman, *ibid.* 37, 364 (1976); W. Hanke, J. Hafner, and H. Bilz, *ibid.* 37, 1560 (1976); S. K. Sinha and B. N. Harmon, in *Supercontivity of d and f-band Metals*, edited by D. H. Douglass (Plenum, New York and London, 1976); C. M. Varma and W. Weber, Phys. Rev. Lett. 39, 1094 (1977)
[8]H. G. Smith, N. Wakabayashi, R. M. Nicklow, and S. Mihailovich, *Proceedings in Low Temperature Physics*, edited by K. D. Timmerhaus, W. J. O'Sullivan, and E. F. Hammel (Plenum, New York, 1974), LT13, Vol. 3.
[9]H. F. Bezdek, R. F. Schmunk, and F. Feingold, Phys. Status Solidi 42, 275 (1970).
[10]S. K. Sinha, T. O. Brun, L. D. Muhlestein, and J. Sakurai, Phys. Rev. B 1, 2430 (1970).
[11]C. Stassis, J. Zarestky, and B. N. Harmon, Solid State Commun. 26, 161 (1978).
[12]J. Goldak, L. T. Lloyd, and C. S. Barrett, Phys. Rev. 144, 478 (1966).
[13]S. C. Moss, D. T. Keating, and J. D. Axe, Solid State Commun. 13, 1465 (1973).
[14]E. S. Fisher and M. H. Manghnani, J. Phys. Chem. Solids 32, 657 (1971).
[15]T. H. K. Barron, *Proceedings of the International Conference on Lattice Dynamics*, edited by R. F. Wallis (Pergamon, Oxford, 1963); R. A. Cowley, Adv. Phys. 12, 421–480 (1963).
[16]W. Cochran and R. A. Cowley, Handb. Phys. 25/2a (1967); D. C. Wallace, *Thermodynamics of Crystals* (Wiley, New York, 1972).
[17]J. C. K. Hui and P. B. Allen, J. Phys. C 8, 2923 (1975).
[18]A. P. Miiller and B. N. Brockhouse, Can. J. Phys. 49, 704 (1971).
[19]R. E. DeWames, T. Wolfram, and G. W. Lehman, Phys. Rev. 138, A717 (1965).
[20]L. J. Raubenheimer and G. Gilat, Phys. Rev. 157, 586 (1967).
[21]See, for instance, R. A. Cowley, Rep. Prog. Phys. 31, 123 (1968).
[22]M. Shimizu and A. Katsuki, J. Phys. Soc. Jpn. 19, 1856 (1964).
[23]G. Grimvall, Phys. Chem. Solids 29, 1221 (1968).
[24]G. B. Skinner, Ph.D. thesis (Ohio State University, 1951).
[25]J. L. Scott, Oak Ridge National Laboratory Report No. ORNL-2328, 1957 (unpublished).
[26]J. P. Coughlin and E. G. King, J. Am. Chem. Soc. 72, 2262 (1950).
[27]N. Wakabayashi (private communication).
[28]G. Jepsen, O. K. Andersen, and R. A. Mackintosh, Phys. Rev. B 12, 3084 (1975).